Biochemical Pharmacology, Vol. 57, pp. 1037–1046, 1999.

ISSN 0006-2952/99/$–see front matter
PII S0006-2952(99)00022-2

pH and Drug Resistance. I. Functional Expression of Plasmalemmal V-type H^+-ATPase in Drug-Resistant Human Breast Carcinoma Cell Lines

Raul Martínez-Zaguilán, Natarajan Raghunand, Ronald M. Lynch, William Bellamy, Gloria M. Martinez, Bertha Rojas, Douglas Smith, William S. Dalton† and Robert J. Gillies‡*

Departments of Biochemistry, Physiology, Pathology and Pharmacology, University of Arizona Health Sciences Center, Tucson, AZ 85724-5042, U.S.A.

ABSTRACT. A major obstacle for the effective treatment of cancer is the phenomenon of multidrug resistance (MDR) exhibited by many tumor cells. Many, but not all, MDR cells exhibit membrane-associated P-glycoprotein (P-gp), a drug efflux pump. However, most mechanisms of MDR are complex, employing P-gp in combination with other, ill-defined activities. Altered cytosolic pH (pH_i) has been implicated to play a role in drug resistance. In the current study, we investigated mechanisms of pH_i regulation in drug-sensitive (MCF-7/S) and drug-resistant human breast cancer cells. Of the drug-resistant lines, one contained P-gp (MCF-7/DOX; also referred to as MCF-7/D40) and one did not (MCF-7/MITOX). The resting steady-state pH_i was similar in the three cell lines. In addition, in all the cell lines, HCO_3^- slightly acidified pH_i and increased the rates of pH_i recovery after an acid load, indicating the presence of anion exchanger (AE) activity. These data indicate that neither Na^+/H^+ exchange nor AE is differentially expressed in these cell lines. The presence of plasma membrane vacuolar-type H^+-ATPase (pmV-ATPase) activity in these cell lines was then investigated. In the absence of Na^+ and HCO_3^-, MCF-7/S cells did not recover from acid loads, whereas MCF-7/MITOX and MCF-7/DOX cells did. Furthermore, recovery of pH_i was inhibited by bafilomycin A_1 and NBD-Cl, potent V-ATPase inhibitors. Attempts to localize V-ATPase immunocytochemically at the plasma membranes of these cells were unsuccessful, indicating that V-ATPase is not statically resident at the plasma membrane. Consistent with this was the observation that release of endosomally trapped dextran was more rapid in the drug-resistant, compared with the drug-sensitive cells. Furthermore, the drug-resistant cells entrapped doxorubicin into intracellular vesicles whereas the drug-sensitive cells did not. Hence, it is hypothesized that the measured pmV-ATPase activity in the drug-resistant cells is a consequence of rapid endomembrane turnover. The potential impact of this behavior on drug resistance is examined in a companion manuscript. BIOCHEM PHARMACOL **57**;9:1037–1046, 1999. © 1999 Elsevier Science Inc.

KEY WORDS. MDR; P-glycoprotein; H^+-ATPase; SNARF-1; intracellular pH; MCF-7; cancer cells; vacuolar pH

A major barrier for the effective treatment of cancer is the phenomenon of MDR§ exhibited by tumor cells [1, 2]. While some mechanisms of resistance allow cells to survive exposure to a single agent, the phenomenon of MDR confers upon cells the ability to withstand exposure to lethal doses of many structurally unrelated antineoplastic agents. Drugs commonly involved in MDR are generally natural products or their derivatives, e.g. anthracyclines, *Vinca* alkaloids, epipodophyllotoxins, and actinomycin D (reviewed in Ref. 3). Many of these are weak bases, such as the anthracycline derivatives MITOX and DOX, and their distribution thus would be affected by pH gradients (see Ref. 4). A common feature of MDR cells is a net decrease in the intracellular accumulation of drugs. MDR has been strongly linked to the overexpression of membrane-associated drug efflux pumps, P-gp or multidrug resistance-associated proteins (MRP) [5].

Alterations in pH_i homeostasis also have been implicated in drug resistance. MDR cells are sometimes observed with a more alkaline pH_i than their drug-sensitive counterparts, yet this observation is inconsistent, indicating that

* Current address: Department of Physiology, Texas Tech University Health Sciences Center, 3601 4th St., Lubbock, TX 79430.

† Current address: Moffitt Cancer Center, 12902 Magnolia Drive, Tampa, FL 33612.

‡ Corresponding author: Dr. Robert J. Gillies, Department of Biochemistry, University of Arizona Health Sciences Center, 1501 N. Campbell Ave., Tucson, AZ 85724-5042. Tel. (520) 626-5050; FAX (520) 626-5051; E-mail: Gillies@u.arizona.edu

§ *Abbreviations*: AE, anion exchanger; AM, acetoxymethyl ester; CPB, cell perfusion buffer; DOX, doxorubicin; MDR, multidrug resistant/resistance; MITOX, mitoxantrone; NHE, Na^+/H^+ exchange; P-gp, P-glycoprotein; pH_e, extracellular pH; pH_i, cytosolic pH; pH_v, endosomal/lysosomal pH; R, ratio; R_{max}, maximum ratio; R_{min}, minimum ratio; and SNARF-1, carboxy-seminaphthorhodafluor-1.

Received 20 November 1997; accepted 28 September 1998.

other processes must be involved [6–12]. The pH_i of mammalian cells is mainly regulated by the collaboration between Na^+/H^+ exchange and HCO_3^--based transport mechanisms (reviewed in Refs. 13 and 14). In some specialized cells such as kidney cells, gastric cells, hepatocytes, macrophages, and osteoclasts, vacuolar (V)-type H^+-ATPase activity has been demonstrated at the plasma membrane (pmV-ATPase) [15, 16]. Additionally, some human tumor cells also exhibit pmV-ATPase activity [17], and this pump is overexpressed in some MDR cells [18, 19]. A functional role for pmV-ATPase activity in tumor cells is not yet known.

In this study, we investigated the mechanisms of pH regulation in drug-sensitive and drug-resistant human breast cancer cell lines. The MCF-7 line was used as the experimental model because a number of clones derived from the parental cell line are available with various degrees and different mechanisms of drug resistance [20]. The parental drug-sensitive MCF-7 cell line (MCF-7/S) was used along with P-gp-negative mitoxantrone-resistant (MCF-7/MITOX) cells or P-gp-positive doxorubicin-resistant (MCF-7/DOX; also referred to as MCF-7/D40) cells. Although these cell lines were independently derived via stepwise increases in the concentration of each drug, respectively, each cell line exhibits a significant amount of cross-resistance [20].

The current experiments involved measurements of pH_i using the fluorescence of SNARF-1 [21, 22]. Additionally, pH regulation of these same cell lines has been examined in tumors *in vivo* [23]. Consistent with other tumors, the pH_e of all three cell lines decreased as a function of increased tumor size. The pH_i of the drug-sensitive tumors decreased concomitant with the decrease in pH_e, such that the pH gradient (ΔpH) remained constant. In contrast, the pH_i of the drug-resistant tumors remained constant, leading to an increase in the ΔpH with increasing tumor size. Thus, there are differences in the regulation of pH_i *in vivo* between the current drug-resistant and drug-sensitive tumor cell lines.

MATERIALS AND METHODS

Buffers and Chemicals

CPB contained the following: 0.35 mM Na_2HPO_4, 110 mM NaCl, 0.44 mM KH_2PO_4, 5.4 mM KCl, 1 mM $MgSO_4$, 1.3 mM $CaCl_2$, 25 mM HEPES, 5 mM glucose, and 2 mM L-glutamine at a pH of 7.15 at 37°. When required, CPB was supplemented with $NaHCO_3$. Organic components were added the day of experimentation in order to avoid bacterial contamination. The fluorescence ion indicators SNARF-1 and coumarin-dextran were purchased from Molecular Probes. DOX was obtained from Adria Laboratories; MITOX was from Lederle/Cyanamid. All other chemicals were obtained from the Sigma Chemical Co., unless otherwise noted.

Cell Culture

The MCF-7 parental cell line was obtained from the American Type Culture Collection, and were cultured as described previously [20]. Cells were grown in T-75 culture flasks and passed bi-weekly at an inoculation density of 2×10^5 cells/75-cm^2 flask. The cells were cultured in RPMI 1640 medium, supplemented with 10% Nu-serum (Collaborative Research), 10 mM HEPES (Organic Chemicals), 24 mM $NaHCO_3$, 0.1% (v/v) penicillin, 0.1% streptomycin, and 0.1% L-glutamine (GIBCO), pH 7.4, at 37°. These cells were maintained in a 5% CO_2 atmosphere at 37°. Selection of MITOX- or DOX-resistant cell lines was achieved as described previously [20]. Briefly, the parental MCF-7 cell line was exposed to either DOX or MITOX at initial concentrations of 1×10^{-8} M. Fresh drug was added three times per week. As allowed by cell growth, the concentration of each drug was slowly increased in a multiple-step procedure, over a period of several months (*ca.* 30 months to reach a maximum concentration of 4×10^{-7} M, representing a 40-fold increase and full development of the DOX-resistant variant). The MITOX-resistant cell line was selected in a similar fashion by increasing the MITOX concentration from 1×10^{-8} M to 8×10^{-8} M, over a period of 6 months. These cell lines have been fully characterized for growth characteristics, P-gp, chromosome analysis, and drug influx/efflux [20]. These cells are chronically cultured in media containing the highest indicated concentration of their respective drug.

Fluorometric pH_i Measurements

pH_i was determined by the fluorescence of SNARF-1, as described previously [22]. Briefly, cells were inoculated into 60-mm Petri dishes containing 9 × 22-mm cover slips at a density of 2×10^5 cells/60-mm dish in their growing medium, in the 5% CO_2 incubator for 48 hr. Two cover slips (with attached cells) were then transferred to a 60-mm Petri dish containing 7 μM SNARF-1(AM) in CPB, pH 7.15, and incubated for 30 min at 37°. The AM form of SNARF-1 is lipophilic and cell-permeant. Cytosolic esterases hydrolyze SNARF-1(AM), trapping the impermeant free acid form of the dye in the cytosol. Following this incubation, the cover slips were transferred to a 60-mm Petri dish containing CPB without dyes and incubated in a 5% CO_2 atmosphere for 30 min, to allow for complete ester hydrolysis of the dyes. The two cover slips were then placed back-to-back in a holder and put in a quartz cuvette in the spectrofluorometer, which is equipped with a flow-through device for sample perfusion. The cover slips were perfused continuously at 3 mL/min. Sample temperature was maintained by keeping both the water jacket and the perfusion medium at 37° using a circulating water bath (Lauda model RM 20, Brinkmann Instruments).

All fluorescence measurements were performed in an SLM8000C fluorometer (SLM) using 4-nm bandpass slits and an external rhodamine standard as a reference. Data

TABLE 1. *In vitro* and *in situ* calibration parameters for fluorescent dyes

	pK_a	R_{min}	R_{max}	S_{f2}/S_{b2}
SNARF				
In vitro	7.61 ± 0.08	0.46 ± 0.01	3.63 ± 0.35	0.82 ± 0.06
MCF-7/S	7.83 ± 0.10	0.45 ± 0.01	2.50 ± 0.27	0.82 ± 0.06
MCF-7/DOX	7.60 ± 0.08	0.49 ± 0.01	2.08 ± 0.17	0.89 ± 0.05
MCF-7/MITOX	7.68 ± 0.16	0.44 ± 0.01	2.13 ± 0.16	0.92 ± 0.05
Coumarin-dextran				
In vitro	6.70 ± 0.02	0.010 ± 0.002	6.05 ± 0.02	

Valure are means ± SD from calibrations performed using at least 15 different pH values.

were collected in a continuous acquisition mode in which the excitation and emission modes were alternated as follows: excitation at 534 nm with acquisitions of the emissions at 584, 600, and 644 nm (SNARF-1 conditions). The duration of this cycle was 0.109 min, and it was repeated as often as necessary. Fluorescence data were translated to ASCII format for manipulation and analysis. Ratio values obtained were converted to pH_i by the following equation:

$$pH = pK_a + \log(S_{f2}/S_{b2}) + \log[(R - R_{min})/(R_{max} - R)] \quad (1)$$

where R_{min} and R_{max} represent the 644/584 ratios of the fully protonated and fully deprotonated SNARF-1, respectively. S_{f2} and S_{b2} are the fluorescence values at 584 nm for the deprotonated and protonated forms of the dye, respectively. These are used to correct for the ion sensitivity of the denominator wavelength [22].

Measurement of Endosomal/Lysosomal and Cytosolic pH by Fluorescence

Endosomal/lysosomal and cytosolic pH were measured simultaneously using the fluorescence of 7-hydroxycoumarin conjugated to 70-kDa dextran (coumarin-dextran) and SNARF-1, respectively. Cultures on coverslips were incubated with 0.05 mg/mL of coumarin-dextran for 2–3 hr, which loads both the endosomal and lysosomal compartments to steady state. Then cells were loaded with 0.007 mM SNARF-1(AM) (*vide supra*) for 30 min, followed by 30 min in dye-free buffer to complete ester hydrolysis at 37°. Under these loading conditions, the coumarin-dextran is localized to the endosomes and lysosomes (the E-L compartment) and the de-esterified SNARF-1 is localized to the cytosol [17].

Fluorescence measurements were carried out as above, except that data were collected by sequential acquisition at excitation wavelengths of 352, 370, and 402 nm at an emission wavelength of 448 nm (coumarin-dextran conditions), followed by excitation at 534 nm, collected at emissions of 584, 600, and 644 nm (SNARF-1 conditions). Cycles were repeated every 13.3 sec. For coumarin-dextran, the ratio of fluorescence at excitations of 352 and 402 nm is pH-sensitive, whereas fluorescence at 370 nm is not (isoexcitation point). For SNARF-1, fluorescence at emissions of 584 and 644 nm is pH-sensitive, whereas fluorescence at 600 nm is not (isoemissive point). The ratio values were converted to pH values using standard calibration curves. These conditions were also used to monitor the release of dye (see below). pH recovery rates following an ammonium prepulse were measured as the slope (dpH/dt) between 5 and 8 min following the switch to NH_4Cl-free buffer. This time was chosen to represent the initial phase of pH recovery at a time after all ammonium has left the system. pH_i values during this recovery measurement period were consistently between 6.8 and 7.0.

In Situ *Calibration of Ion Indicators*

We have shown previously that the *in situ* calibration parameters of pH indicators may vary from cell type to cell type, and therefore accurate calibrations are needed to assign pH values *in situ* [22, 24]. The calibration of SNARF-1 was performed as described previously [17]. Briefly, attached (SNARF-1 loaded) cells were perfused with their corresponding high K^+ buffer plus a 6.8 μM concentration of the K^+/H^+ ionophore nigericin and 2 μM valinomycin, which elicits equilibration of cytosolic and extracellular pH, i.e. pH_i of the cells is equal to pH_e. For these experiments, pH_e was varied from pH 6.0 to 8.0. From these *in situ* calibration curves one can obtain *R* values at each pH_e studied. Equation (1) was then solved iteratively using nonlinear least-squares analysis (MINSQ, MicroMath Scientific Software), yielding values of R_{max}, R_{min}, and pK_a for the dye. *In vitro* and *in situ* calibration curves yielded the parameters shown in Table 1. pH_v was estimated from *in vitro* calibration curves and not from *in situ* calibration parameters due to the uncertainty of equilibration of extracellular K^+ with the lysosomal/endosomal compartments. *In vitro* pH values used for calibration were obtained with a Beckman model 71 pH meter, using a Corning glass combination electrode. The electrode was calibrated at two known temperature-controlled pH values, using commercially prepared standards from VWR Scientific.

Measurement of Endosomal Turnover Rates by Dye Release

To estimate endosomal turnover rates, cells on coverslips were incubated with coumarin-dextran as above for 2 hr at 37°. Following this incubation, two coverslips were placed back-to-back in the cuvette, and data were acquired at an emission wavelength of 448 nm and excitation wavelengths of 352, 370, and 402 nm. Then perfusion was begun with CPB. The fluorescence at 370-nm excitation was taken to represent dye concentration, since it is pH-insensitive. The decline in 370-nm fluorescence followed a double exponential curve, with the initial decay from washing adventitial dye off the surface of the cells, and the second component representing release of dye from recycling endosomes. The first component was complete within 5 min of perfusion. Hence, the time-dependent decrease in fluorescence was fit to a single exponential curve beginning 5 min after the start of perfusion. These data were obtained from all three cell lines, as well as from two negative controls: MCF-7/MITOX cells at 4° and MCF-7/MITOX cells in the presence of 0.05 mM Colcemid.

Immunocytochemistry

Cells were fixed in 4% filtered paraformaldehyde, and unreacted fixative was quenched with 25 mM glycine. Then the cells were permeabilized with 0.05% saponin for 15 min. Next the cells were incubated with a 1:10,000 dilution of Mab Fl3.2, which recognizes subunit B of the human V-type H^+-ATPase [25]. This antibody was a gift from M. Forgac, Tufts University. After staining with primary antibody for 45 min, cells were washed, and then incubated with fluorescein-conjugated anti-mouse antibody for an additional 45 min. After washing, the coverslips were mounted on microscope slides with *p*-phenylenediamine dissolved in glycerol, and sealed. Images were obtained on an Olympus IMT-2 epifluorescence microscope equipped with achromatic lenses and a liquid-cooled Photometrics CCD camera with a Tektronics (TEK-512) 512 × 512 pixel chip. Images were captured using Photometrics PMIS imaging software running on a 80486 computer with 32 Mb RAM. Image processing was performed using a Silicon Graphics Personal IRIS for image and graphics analysis and Silicon Graphics IRIS INDIGO 3000xs for computation. To image in three dimensions, the cell image was aligned in the camera field, and the image was viewed through emission filters selected for the fluorophores of interest. A computer controlled the microscope focus and the shutter of a camera. A magnetic eddy current position sensor provided precise information to the computer regarding the relative position of the objective from the sample. A series of images were collected at planes of focus minimally spaced 0.25 μm apart. Images from different focal planes through the cell were deconvolved in three dimensions using a point-spread function to provide information regarding each object in all planes of focus [26].

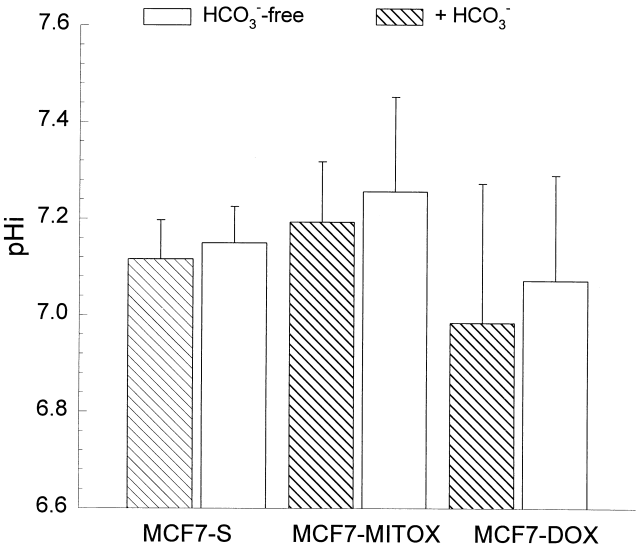

FIG. 1. Steady-state pH_i in MCF-7/S, MCF-7/MITOX, and MCF-7/DOX cell lines, in the presence and absence of HCO_3^-. Cells were grown onto cover slips for 72 hr before experiments. Thereafter, two cover slips containing cells (at subconfluence) were loaded with SNARF-1 and prepared for fluorescence experiments as described in Materials and Methods. Subsequently, two cover slips were placed (back-to-back) into a holder/perfusion device as described previously [22]. Cells were perfused continuously with CPB at a rate of 3 mL/min, and steady-state pH_i was measured. Data represent the means ± SD of nine independent measurements.

DOX Localization by Confocal Microscopy

MCF-7 cells exposed to DOX were visualized using a Zeiss model 210 confocal microscope equipped with a HeNe laser. Cells were seeded onto sterile glass coverslips at a density of 1×10^6 cells/coverslip and allowed to attach overnight prior to drug exposure. The coverslips were then placed into a modified Dvorak-Stotler controlled-environment culture chamber (Nicholson Precision Instruments, Inc.) maintained at 37° and exposed to 1 μM doxorubicin for 30 min.

RESULTS

Steady-State pH_i, Bicarbonate Transport, and Sodium-Proton Exchange

The pH_i values of drug-sensitive (MCF-7/S) and drug-resistant (MCF-7/MITOX, MCF-7/DOX) human breast carcinoma cell lines were determined under conditions where the HCO_3^--based transporting mechanisms are either inactive (absence of HCO_3^-) or active (presence of HCO_3^-). Cells were perfused in the cuvette at a rate of 3 mL/min with CPB in the presence or absence of HCO_3^- at a pH_e of 7.15. This pH_e was used because it best approximates the pH_e experienced *in vivo* [23]. As shown in Fig. 1, the steady-state pH_i of all three cell lines was higher in the absence of HCO_3^-. Furthermore, the differences in steady-state pH_i between the three cell lines were not significant, either in the presence or absence of HCO_3^-. Therefore,

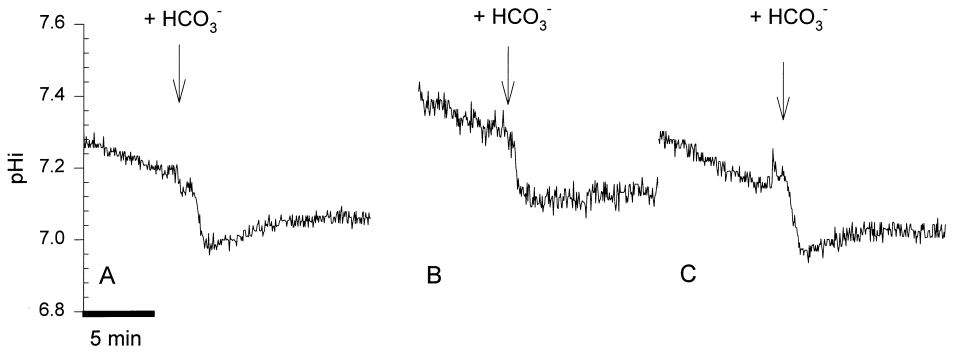

FIG. 2. Effect of HCO_3^- on pH_i in MCF-7/S (A), MCF-7/MITOX (B), and MCF-7/DOX (C) cell lines. Cells were handled as described for Fig. 1. Perfusion was begun with HCO_3^--free CPB. At the time indicated (arrow), the perfusate was exchanged for CPB containing HCO_3^-. Data are representative of five independent experiments for each cell line.

differences in steady-state pH_i cannot explain the differences in drug-sensitivity exhibited by these cell lines. Although HCO_3^- did not affect the pH_i significantly, it is still possible that HCO_3^--based H^+ transporting mechanisms participate in pH_i regulation in these cell types [27, 28].

The activity of HCO_3^- transporting mechanisms vis-à-vis the MDR phenotype was then examined. Figure 2 shows that addition of HCO_3^- to HCO_3^--depleted cells uniformly resulted in a rapid decrease in pH_i of *ca.* 0.2 pH units in all cell types. The magnitude of this decrease was not different among the three cell lines (cf. Fig. 2, A, B, and C). These data indicate that all three of these cell lines express comparable levels of a HCO_3^-/Cl^- exchanger of the AE family that works to acidify the cytosol. This was confirmed by monitoring the rate of pH_i recovery from an NH_4Cl-induced acid load in the presence and absence of HCO_3^- [13]. As shown in Fig. 3, the rate of pH_i recovery after an acid load was similar in all three cell lines, whether or not HCO_3^- was present (solid lines) or absent (dotted lines). In the absence of HCO_3^-, the predominant pH-regulatory mechanism was presumed to be Na^+/H^+ exchange (NHE-1). As shown in these figures, the rate of recovery in the presence of HCO_3^- was much greater, compared with its absence, indicating that AE is much more active in these cell lines, compared with NHE-1. Results from a number of similar experiments are presented in Table 2, and indicate that neither NHE activity nor AE activity was associated with the MDR phenotype.

Vacuolar (V)-type H^+-ATPase Activity at the Plasma Membrane of Drug-Resistant Cell Lines

Neither Na^+/H^+ exchange nor HCO_3^--based transporting mechanisms are related to MDR in this system. A third type of pH-regulatory activity has been observed in some tumor cells, viz. plasmalemmal vacuolar-type H^+-ATPase (pmV-ATPase) activity. To measure pmV-ATPase activity, acid loading experiments were performed in the absence of both HCO_3^- and Na^+ to inactivate both AE and NHE. Acid loads were given at a pH_e of 8.0 in order to prevent the nadir of pH_i following NH_4Cl washout from going below 6.8, where pmV-ATPase activities are reduced [17]. As shown in Fig. 4A, under these conditions MCF-7/S cells did

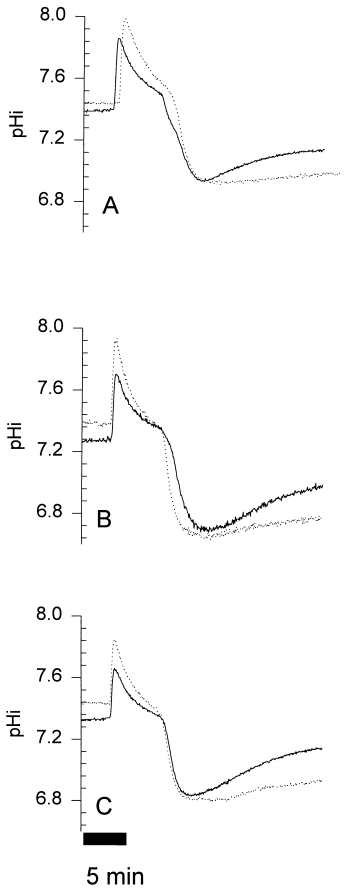

FIG. 3. Effect of NH_4Cl on pH_i in the absence and presence of HCO_3^-. MCF-7/S (A), MCF-7/MITOX (B), and MCF-7/DOX (C) cells were handled as described in the legend to Fig. 1. Cells were perfused with CPB in the absence (dotted lines) or presence (solid lines) of HCO_3^-. After 3 min, perfusate was exchanged for one containing NH_4Cl in normal or HCO_3^--free CPB, respectively. Five minutes later, perfusate was exchanged back to the original CPB (NH_4Cl-free). Data are representative of six independent experiments for each cell line.

TABLE 2. Summary of results: Rates of pH_i recovery

Condition	dpH/dt (10^{-3} pH unit/min)		
	MCF-7/S	MCF-7/DOX	MCF-7/MITOX
HCO_3^--free + Na^+	6.65 ± 2.1 (6)	8.6 ± 2.9 (6)	10.7 ± 4.8 (6)
HCO_3^- + Na^+	25.1 ± 7.3 (6)	26.5 ± 5.1 (6)	28.5 ± 6.8 (6)
HCO_3^- & Na^+-free	2.45 ± 3.3 (9)	27.4 ± 9.4 (9)	24.1 ± 7.8 (9)
+ Bafilomycin A, 1 μM	NA	−2.8 ± 1.4 (3)	−5.3 ± 3.6 (4)
+ NBD-Cl 50 μM	NA	−7.7 ± 2.5 (6)	−10.3 ± 4.5 (6)

Values are means ± SEM of the number of experiments indicated in parentheses. dpH/dt was obtained from a plot of dpH versus time between 5 and 8 min following removal of 10 mM NH_4Cl.
NA = not applicable

not recover from NH_4Cl-induced acid loads, whereas the drug-resistant cell lines MCF-7/MITOX and MCF-7/DOX did. As explained in Materials and Methods, pH_i recovery rates in experiments such as the ones shown in Fig. 4A were measured as the slope (dpH/dt) between 5 and 8 minutes following the switch to NH_4Cl-free buffer. From a number of experiments similar to those shown in Fig. 4A, we have estimated that the rates of pH_i recovery are slightly faster in MCF-7/DOX than in MCF-7/MITOX cells, yet these differences were not significant (Table 2). The pH_i recovery was mediated via V-H^+-ATPase, since it was inhibited by bafilomycin A_1 and NBD-Cl (panels B and C of Fig. 4, Table 2). These observations indicate that pmV-ATPase activity is functionally expressed in both P-gp-positive and P-gp-negative drug-resistant cell lines, and not in the drug-sensitive cell line.

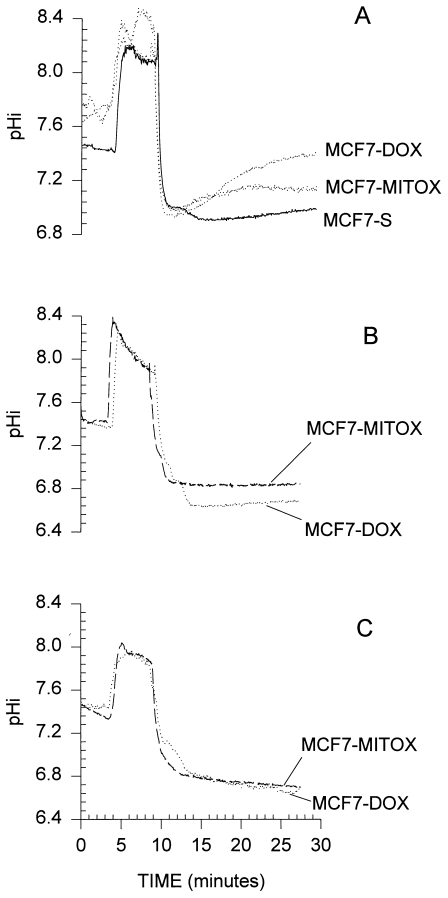

FIG. 4. (A) pH_i recovery in the absence of Na^+ and HCO_3^-. MCF-7/S, MCF-7/MITOX, and MCF-7/DOX cells were handled as described in the legend of Fig. 1. Cells were perfused for 3 min with HCO_3^--free CPB at pH_e = 8.0. Thereafter, perfusate was exchanged for CPB supplemented with 10 mM NH_4Cl, and continuously perfused for 5 min. At the end of this period of time, perfusate was exchanged for HCO_3^-- and Na^+-free CPB. (B) Effect of bafilomycin A_1 on pH_i recovery. Cells were handled as described in (A), except that the buffers contained 1 μM bafilomycin A_1 from beginning to end of the experiment. (C) Effect of NBD-Cl on pH_i recovery. Cells were handled as described in (B), except that 50 μM NBD-Cl was used instead of bafilomycin A_1.

Steady-State pH_v in Drug-Sensitive and Drug-Resistant Cell Lines

The presence of plasmalemmal V-H^+-ATPase at the plasma membranes in MDR cells, but not in sensitive cells, might be due to overexpression of V-H^+-ATPases and/or mistargeting. Previous studies by Ma and Center [19] have shown that the C-subunit of V-H^+-ATPase is overexpressed in human leukemia cells expressing the MDR phenotype. If V-ATPase were overexpressed, it might alter the steady-state pH of the endosomes or lysosomes (pH_v). Fig. 5B shows that the steady-state pH_v was not different between sensitive and resistant cell lines. Moreover, Fig. 5A shows that addition of NH_4Cl did not affect the endosomal/lysosomal compartment, suggesting that the H^+-buffering capacities in these entities are extremely high. Previous studies have shown that the "active" H^+-buffering capacity in endosomes/lysosomes is cell-type dependent and can be as high as 2.75 M H^+/pH unit [17]. These data suggest that neither the pH_v nor the H^+-buffering capacity of the endosomal/lysosomal compartments can explain the MDR phenotype.

Immunocytochemistry using monoclonal or polyclonal antibodies against the "B" subunit of V-ATPase has failed to show localization of V-ATPase at the plasma membrane, although numerous intracellular structures are labeled (e.g. Fig. 6). These data were obtained regardless of how the cells were prepared on coverslips (i.e. with fibronectin, with serum, at low or high density). These data are also consistent with those obtained from metastatic C8161 melanoma

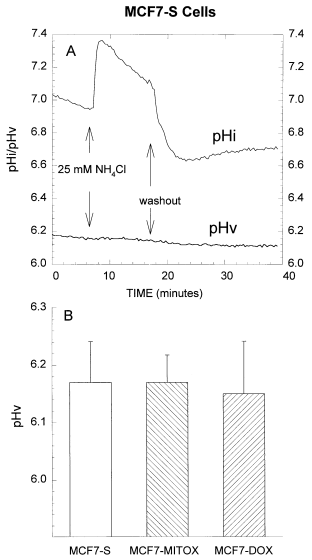

FIG. 5. (A) Effect of NH_4Cl on endosomal/lysosomal pH (pH_v) and cytosolic pH (pH_i) in MCF-7/S cells. Cells were co-loaded with SNARF-1 and coumarin-dextran, as described in Materials and Methods. Coverslips containing cells were transferred to the fluorometer cuvette, and perfusion was begun with HCO_3^--free CPB, at a pH_e of 7.15. At the time indicated, perfusate was exchanged for one containing 10 mM NH_4Cl. Data are representative of six experiments. (B) Steady-state pH_v. MCF-7/S, MCF-7/MITOX, and MCF-7/DOX cells were co-loaded with SNARF-1 and coumarin-dextran, and their pH_i and pH_v were monitored as in (A). Steady-state pH_v was measured during the first 6 min of the experiment. Data represent the means ± SD of six independent experiments.

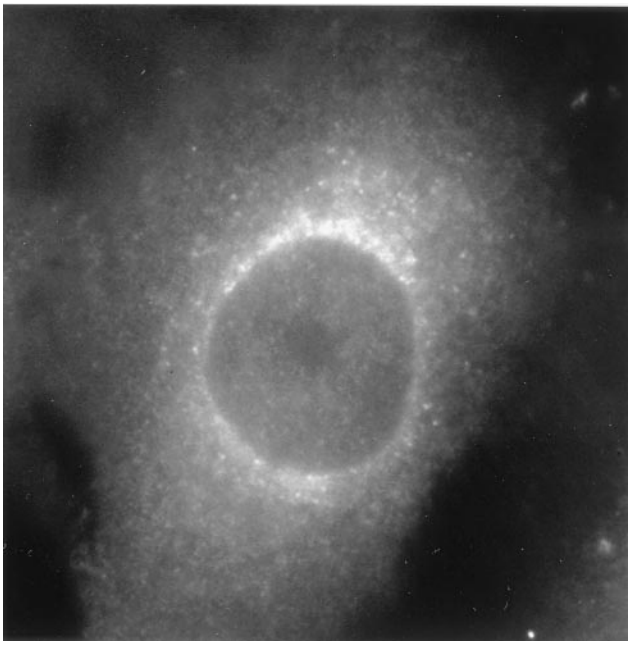

FIG. 6. Immunocytochemistry of MCF-7/DOX cells labeled with V-ATPase antibody. MCF-7/DOX cells were grown on coverslips, fixed and stained with monoclonal antibody Fl3.2, which recognizes the "B" subunit of V-ATPase. This figure is representative of dozens of experiments under a variety of conditions, varying serum, growth status, fibronectin, and pH. MCF-7/MITOX and MCF-7/S cells showed similar staining patterns.

cells (unpublished observations), and they indicate that V-ATPase is not statically resident at the plasma membrane. Thus, the measured V-ATPase activity (i.e. H^+ extrusion in the absence of Na^+ and HCO_3^-) might result from the dynamic exocytosis of acidic vesicles and not the static residence of V-ATPase pumps at the cell surface.

Endosomal Turnover in Drug-Sensitive and Drug-Resistant Cells

Endosomal turnover was investigated by monitoring the release of endosomally trapped coumarin-dextran. Coumarin-dextran has an acidic pK_a, two pH-sensitive wavelengths (352 and 402 nm), and a pH-insensitive isoexcitation wavelength (370 nm). In these experiments, cells on coverslips were allowed to endocytose coumarin-dextran for 2–3 hr, after which they were placed in the cuvette and perfused with CPB while monitoring fluorescence at pH-sensitive and -insensitive wavelengths. Figure 7A illustrates the fluorescence at all three wavelengths prior to and during perfusion of MCF-7 cells loaded with coumarin-dextran. As shown in this figure, there was a dramatic drop in fluorescence in all three wavelengths within 1 min of the beginning of perfusions (arrow). Following this initial drop, the fluorescence at the isoemissive wavelength (370 nm) declined slowly, whereas the fluorescence intensities of the other wavelengths changed more rapidly, indicating that the pH of the environment of the dye was changing with kinetics distinct from the drop in dye concentration. The rate of decline in isoemissive fluorescence at 370 nm 10 min after the start of perfusion was taken to represent the rate at which dye is exocytosed from the endosomal/lysosomal store. This interpretation is supported by the observation that dye release was inhibited by low temperature (4°) and by 0.05 to 0.1 μM Colcemid (T and C, respectively, in Fig. 7C). Dye was released more rapidly from the drug-resistant cells. This is shown in Fig. 7B, which plots the fluorescence as a function of time in MITOX-resistant and -sensitive cells. The compiled data are shown in Fig. 7C, which shows a significantly ($P < 0.005$) higher rate of dye leakage from MITOX- (M) and DOX- (D) resistant cells compared with the parental drug-sensitive (S) cells.

DOX Sequestration in Vesicles in Drug-Resistant Cells

DOX is endogenously fluorescent. When this drug was incubated with MCF-7/DOX or MCF-7/MITOX cells, it was excluded from the nucleus and sequestered in cytoplasmic vesicles (e.g. Fig. 8). This pattern persisted for approximately 1 hr, after which time, drug was expelled completely from the cells. This is in contrast to the pattern observed in MCF-7/S cells, which stained uniformly throughout the cytoplasm and the nucleus (data not shown). *In toto*, these observations prompt the hypothesis

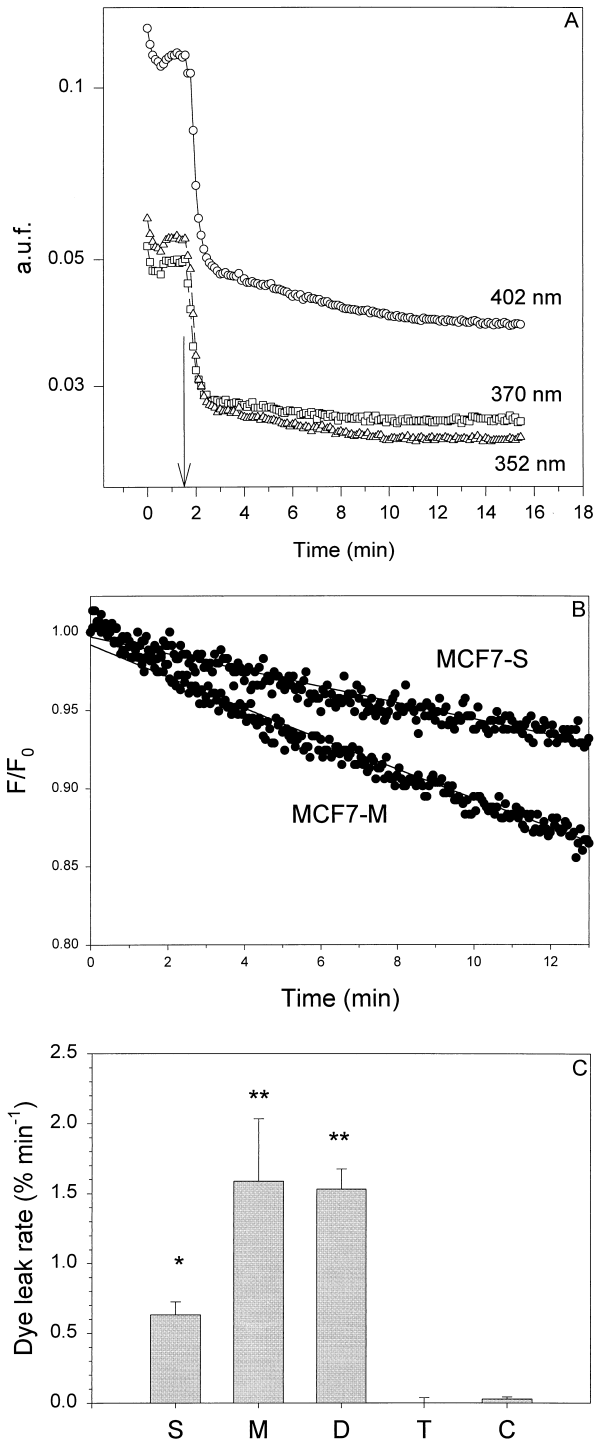

FIG. 7. (A) Fluorescence of coumarin-dextran during fluorophore-free perfusion. MCF-7/DOX cells were loaded for 2 hr with coumarin-dextran as described in Materials and Methods, after which time they were placed in a fluorometer cuvette, and fluorescence was monitored sequentially at excitation wavelengths of 352, 370, and 402 nm. Perfusion with fluorophore-free CPB was begun at 90 sec (arrow). Note that data are plotted semi-logarithmically and that fluorescence values at all three wavelengths decreased to different degrees. (B) Exocytosis in MCF-7/S and MCF-7/MITOX cells. Data were obtained as in (A) from MCF-7/S and MCF-7/MITOX cells. Time = 0 was set to 10 min after the beginning of perfusion, and all subsequent fluorescence values (F) were normalized to the value at this time (F_0). Dots indicate raw data, and lines represent the fitted first-order exponential slopes. (C) Leak rate. Data were obtained as in (A) from MCF-7/sec(S), MCF-7/MITOX (M), and MCF-7/DOX (D) cells, as well as from MCF-7/MITOX cells perfused with CPB at 4° (T) or in the presence of 50 μM Colcemid (C). Data (means ± SD) were from a minimum of three (T, C) and a maximum of 18 (S, M, D) independent measurements per condition. Leak rate is expressed as percent per minute, determined from time constants of first-order exponential fits to data as in (B). For S, $P < 0.005$ relative to all others (*). For M and D, $P < 0.001$ relative to negative controls (T, C), and $P < 0.005$ relative to S (**).

that weakly basic chemotherapeutic drugs are sequestered in a recycling acidic vesicle compartment and thus are removed rapidly from the cytosol. The implications of this are investigated in the companion manuscript [4].

DISCUSSION

Steady-State pH_i in MDR and Sensitive Cells

It has been suggested that reduced intracellular accumulation of drugs could be due to alkaline-inside pH gradients. For example, the pH_i of Chinese hamster ovary (CHO) cells resistant to colchicine (CH^RC5 cells) and that of Chinese hamster lung (CHL) cells resistant to actinomycin

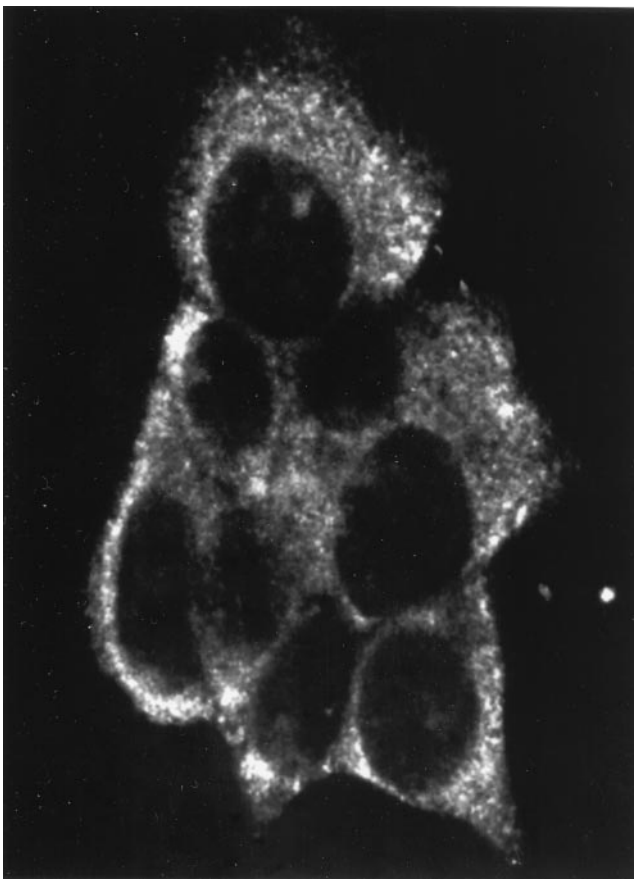

FIG. 8. DOX localization by confocal microscopy. Intracellular distribution of DOX in MCF-7/DOX cells incubated in the presence of 1 μM DOX for 30 min at 37° (see text for details).

D (DC3F-ADX) is approximately 0.15 pH units higher than their parental (i.e. drug-sensitive) cell lines [9]. A trend of higher pH_i with increasing degrees of MDR also has been shown in a series of human lung tumor cell lines [10] and breast cancer cells [29]. Moreover, Roepe [30] has also shown that increased steady-state levels of chemotherapeutic drug efflux from MDR myeloma cells were correlated with intracellular alkalinization. In the same cell lines as in the current study, we have observed that the pH gradient *in vivo* is larger for the drug-resistant lines compared with the drug-sensitive lines, only at large tumor volumes [23]. Consistent with this, data from the current study indicate that, at a pH_e of 7.15, there were no significant differences in steady-state pH_i between drug-sensitive (MCF-7/S) and drug-resistant (MCF-7/DOX or MCF-7/MITOX) cell lines, regardless of the presence or absence of HCO_3^- (Fig. 1). Similarly, a lack of correlation between MDR and pH_i has been shown in MCF-7/S and Adriamycin-resistant MCF-7 cell lines [6] and in a series of sensitive and MDR human lung carcinoma cells [7]. Moreover, neither human HeLa-Pur^{RII} cells resistant to puromycin nor KB-Cl human cells resistant to colchicine exhibit a higher pH_i when compared with their sensitive parental cell lines [9]. Furthermore, Altenberg *et al.* [8] have shown that acute changes in intra- or extracellular pH do not affect P-gp-dependent drug efflux in MDR cell lines. Therefore, MDR can occur in cells with low, normal, or high pH_i. The reasons for these apparent discrepancies are unclear. It is unlikely that the lack or presence of correlation of MDR with pH_i is due to different experimental conditions but rather to the existence of multiple mechanisms of MDR. For example, Soto *et al.* [11] have found that P-gp-overexpressing murine leukemia cell lines do not have elevated pH_i, whereas P-gp negative drug-resistant cells have elevated pH_i compared with the parental drug-sensitive L1210 cell line. These data suggest that both elevated pH_i and P-gp can contribute to drug resistance in these cell lines. In the present study, we found no differences in steady-state pH_i between cells that express P-gp (MCF-7/DOX) and cells that do not (MCF-7/MITOX and MCF-7/S). This is in contrast to Roepe *et al.* [12], who observed a decrease in AE activity (and elevated pH_i) with increased P-gp transfection copy number. Differences in the activity of NHE or AE are unlikely to be related to drug resistance in the current system. Differences in NHE activity are unlikely to be involved in the MDR phenotype since, in the presence of Na^+ and in the absence of HCO_3^-, both the steady-state pH_i and the rates of pH_i recovery from acid loads were similar between drug-resistant (MCF-7/DOX and MCF-7/MITOX) and drug-sensitive (MCF-7/S) cell lines (Figs. 2 and 3). Previous studies have suggested that the differences in steady-state pH_i observed in some MDR cells could be explained by differences in the activity of NHE, since pH_i recovery was suppressed by amiloride [9]. However, those experiments were performed using the pH indicator BCECF, whose fluorescence is quenched by amiloride [27]. Thus, it is possible that the suppression of the pH_i recovery upon amiloride treatment was artifactual. This suggestion is further supported by the observation that amiloride does not reverse MDR [9]. Furthermore, the magnitude of the pH_i decrease induced by amiloride does not correlate with the degree of reversal of the MDR phenotype in a series of colon carcinoma cells with various degrees of MDR but low P-gp expression [31]. Although the mRNA encoding human NHE is overexpressed in MDR cells, the level of overexpression does not correlate with the relative drug resistance or steady-state pH_i [12].

V-type H^+-ATPase Activity in Drug-Resistant Cells

Two of the main pH_i regulatory mechanisms (Na^+/H^+ exchange and HCO_3^--based H^+-transporting mechanisms) are not different among the MCF-7/S, MCF-7/MITOX, and MCF-7/DOX cell lines. However, the drug-resistant cells express V-H^+-ATPase activity in their plasma membranes, whereas the sensitive cells do not. Previous studies have shown that the subunit C of the V-ATPase is overexpressed in HL60 cells resistant to DOX or vincristine [19]. Similar to the current system, one of the resistant lines (HL60/Vinc) exhibits high levels of P-gp, whereas the other (HL60/Adr) does not [18].

MDR and Intracellular Compartments

The current study showed a lack of staining for V-ATPase at the plasma membrane in all cell lines (Fig. 6, for example) and a higher rate of exocytosis in the cell lines exhibiting pmV-ATPase activity (Fig. 7, panels A–C). These observations suggest a role for rapid endomembrane recycling in drug-resistance. This is addressed theoretically in the companion manuscript [4]. Additionally, there is much evidence in the literature to suggest a role of intracellular compartments in resistance to chemotherapeutic drugs. Many anticancer drugs are weak bases or molecules whose binding to cellular structures is pH dependent (e.g. MITOX and DOX have pK_a values of 7.5 and 8.3, respectively). Accumulation of these drugs within cells thus will be affected by transmembrane pH gradients. Thus, if the endosomal/lysosomal pH (pH_v) were more acidic (e.g. by overexpression of V-H^+-ATPases), it would tend to enhance the accumulation of drugs in any of these compartments and reduce drug accumulation in the cytosol or nucleus. This does not seem to be the case in the present system, since the pH_v was not different between drug-sensitive and drug resistant cell lines (Fig. 5). Nevertheless, DOX and daunomycin rapidly accumulate within acidic compartments, and accumulation can be stimulated by raising pH_i [32]. Thus, the current data suggest that acidic vesicles accumulate drugs and are recycled rapidly, resulting in extrusion of drugs and H^+ from the cells. Hence, the apparent activity of V-ATPase at the plasma membrane is an epiphenomenon of rapid endomembrane recycling.

This work was supported by US Army Breast Cancer Initiative Grant DAMD17–94-J-4368.

References

1. Juranka PF, Zastawny RL and Ling V, P-glycoprotein: Multidrug-resistance and a superfamily of membrane-associated transport proteins. *FASEB J* **3:** 2583–2592, 1989.
2. Roninson IB, Molecular mechanism of multidrug resistance in tumor cells. *Clin Physiol Biochem* **5:** 140–151, 1987.
3. Moscow JA and Cowan KH, Multidrug resistance. *J Natl Cancer Inst* **80:** 14–20, 1988.
4. Raghunand N, Martínez-Zaguilán R, Wright SH and Gillies RJ, pH and drug resistance. II. Turnover of acidic vesicles and resistance to weakly basic chemotherapeutic drugs. *Biochem Pharmacol* **57**: 1047–1058, 1999.
5. Gottesman MM and Pastan I, Biochemistry of multidrug resistance mediated by the multidrug transporter. *Annu Rev Biochem* **62:** 385–427, 1993.
6. Lyon RC, Cohen JS, Faustino PJ, Megnin F and Myers CE, Glucose metabolism in drug-sensitive and drug-resistant human breast cancer cells monitored by magnetic resonance spectroscopy. *Cancer Res* **48:** 870–877, 1988.
7. Versantvoort CH, Broxterman HJ, Feller N, Dekker H and Kuiper CMLJ, Probing daunorubicin accumulation defects in non-P-glycoprotein expressing multidrug-resistant cell lines using digitonin. *Int J Cancer* **50:** 906–911, 1992.
8. Altenberg GA, Young G, Horton JK, Glass D, Belli JA and Reuss L, Changes in intra- or extracellular pH do not mediate P-glycoprotein-dependent multidrug resistance. *Proc Natl Acad Sci USA* **90:** 9735–9738, 1993.
9. Boscoboinik D, Gupta RS and Epand RM, Investigation of the relationship between altered intracellular pH and multidrug resistance in mammalian cells. *Br J Cancer* **61:** 568–572, 1990.
10. Keizer HG and Joenje H, Increased cytosolic pH in multidrug resistance human lung tumor cells: Effect of verapamil. *J Natl Cancer Inst* **81:** 706–709, 1989.
11. Soto F, Planells-Cases R, Canaves JM, Ferrer-Montiel AV, Aleu J, Gamarro F, Castanys S, Gonzalez-Ros JM and Ferragut JA, Possible coexistence of two independent mechanisms contributing to anthracycline resistance in leukaemia P388 cells. *Eur J Cancer* **29A:** 2144–2150, 1993.
12. Roepe PD, Wei LY, Cruz J and Carlson D, Lower electrical membrane potential and altered pH_i homeostasis in multidrug-resistant (MDR) cells: Further characterization of a series of MDR cell lines expressing different levels of P-glycoprotein. *Biochemistry* **32:** 11042–11056, 1993.
13. Roos A and Boron WF, Intracellular pH. *Physiol Rev* **61:** 296–434, 1981.
14. Gillies RJ, Martínez-Zaguilán R, Peterson EP and Perona R, The role of intracellular pH in mammalian cell proliferation. *Cell Physiol Biochem* **2:** 159–179, 1992.
15. Swallow CJ, Grinstein S and Rotstein OD, A vacuolar type H^+-ATPase regulates cytoplasmic pH in murine macrophages. *J Biol Chem* **265:** 7645–7654, 1990.
16. Vaananen HK, Karhukorpi E-K, Sunquist K, Wallmark B, Roinine I, Hentune T, Tuukkanen J and Lakkakorpi P, Evidence for the presence of H^+-ATPase types in the ruffled borders of osteoclasts. *J Cell Biol* **111:** 1305–1311, 1990.
17. Martínez-Zaguilán R, Lynch RM, Martinez GM and Gillies RJ, Vacuolar-type H^+-ATPases are functionally expressed in plasma membranes of human tumor cells. *Am J Physiol* **265:** C1015–C1029, 1993.
18. Marquardt D and Center MS, Involvement of vacuolar H^+-adenosine triphosphatase activity in multidrug resistance in HL60 cells. *J Natl Cancer Inst* **83:** 1098–1102, 1991.
19. Ma L and Center MS, The gene encoding vacuolar H^+-ATPase subunit C is overexpressed in multidrug-resistant HL60 cells. *Biochem Biophys Res Commun* **182:** 675–681, 1992.
20. Taylor CW, Dalton WS, Parrish PR, Gleason MC, Bellany WT, Thompson FH, Roe DJ and Trent JM, Different mechanisms of decreased drug accumulation in doxorubicin and mitoxantrone resistant variants of the MCF7 human breast cancer cell line. *Br J Cancer* **63:** 923–929, 1991.
21. Gillies RJ and Martínez-Zaguilán R, Regulation of intracellular pH in Balb/c-3T3 cells: Bicarbonate raises pH via $NaHCO_3$/HCl exchange and attenuates the activation of Na^+/H^+ exchange by serum. *J Biol Chem* **266:** 1551–1556, 1991.
22. Martínez-Zaguilán R, Martinez GM, Lattanzio F and Gillies RJ, Simultaneous measurement of intracellular pH and Ca^{2+} using the fluorescence of SNARF-1 and Fura-2. *Am J Physiol* **260:** C297–C307, 1991.
23. Raghunand N, Altbach MI, van Sluis R, Baggett B, Taylor CW, Bhujwalla ZM and Gillies RJ, Plasmalemmal pH-gradients in drug-sensitive and drug-resistant MCF-7 human breast carcinoma xenografts measured by ^{31}P magnetic resonance spectroscopy. *Biochem Pharmacol* **57**: 309–312, 1999.
24. Gillies RJ, Martínez-Zaguilán R, Martinez GM, Serrano R and Perona R, Tumorigenic 3T3 cells maintain an alkaline intracellular pH under physiological conditions. *Proc Natl Acad Sci USA* **87:** 7414–7418, 1990.
25. Puopolo K, Kumamoto C, Adachi I, Magner R and Forgac M, Differential expression of the "B" subunit of the vacuolar H^+-ATPase in bovine tissues. *J Biol Chem* **267:** 3696–3706, 1992.
26. Carrington WA, Lynch RM, Moore EDW, Isenberg G, Fogarty KE and Fay FS, Superresolution three-dimensional images of fluorescence in cells with minimal light exposure. *Science* **268:** 1483–1487, 1995.
27. Sanchez-Armass S, Martínez-Zaguilán R, Martinez GM and Gillies RJ, Regulation of pH on rat brain synaptosomes. I. Role of sodium, bicarbonate, and potassium. *J Neurophysiol* **71:** 2236–2247, 1994.
28. Martinez-Zaguilan R, Gillies RJ and Sanchez-Armass S, Regulation of pH in rat brain synaptosomes. II. Role of Cl^-. *J Neurophysiol* **71:** 2249–2257, 1994.
29. Altan N, Chen Y, Schindler M and Simon SM, Defective acidification in human breast tumor cells and implications for chemotherapy. *J Exp Med* **187:** 1583–1598, 1998.
30. Roepe PD, Analysis of the steady-state and initial rate of doxorubicin efflux from a series of multidrug-resistant cells expressing different levels of P-glycoprotein. *Biochemistry* **31:** 12555–12564, 1992.
31. Hamilton G, Cosentini EP, Teleky B, Koperna T, Zacheri J, Riegler M, Feil W, Schiessel R and Wenzi E, The multidrug-resistance modifiers verapamil, cyclosporine A and tamoxifen induce an intracellular acidification in colon carcinoma cell lines *in vitro*. *Anticancer Res* **13:** 2059–2063, 1993.
32. Simon S, Roy D and Schindler M, Intracellular pH and the control of multidrug resistance. *Proc Natl Acad Sci USA* **91:** 1128–1132, 1994.